### CONFERENCE PRE-PRINT

# CHANGE OF WALL MATERIAL FROM BERYLLIUM TO TUNGSTEN IN THE NEW ITER BASELINE: PHYSICS BASIS, IMPLICATIONS FOR RESEARCH PLAN AND WALL DESIGNS FOR ITS OPERATIONAL PHASES

A. LOARTE<sup>1</sup>, R. A. PITTS<sup>1</sup>, T. WAUTERS<sup>1</sup>, F. KÖCHL<sup>1</sup>, A. PSHENOV<sup>1</sup>, S.H. KIM<sup>1</sup>, S. PINCHES<sup>1</sup>, J. ARTOLA<sup>1</sup>, S. JACHMICH<sup>1</sup>, M. SCHNEIDER<sup>1</sup>, R. HUNT<sup>1</sup>, S. CARPENTIER-CHOUCHANA<sup>1</sup>, L. CHEN<sup>1</sup>, D. BOILSON<sup>1</sup>, N. CASAL<sup>1</sup>, W. HELOU<sup>1</sup>, Y. KAMADA<sup>1</sup>, A. BECOULET<sup>1</sup>, K. SCHMID<sup>2</sup>, C. ANGIONI<sup>2</sup>, D. FAJARDO<sup>2</sup>, V. BOBKOV<sup>2</sup>, S. BREZINSEK<sup>3</sup>, C. BAUMANN<sup>3</sup>, J. ROMAZANOV<sup>3</sup>, S. RODE<sup>3</sup>, H. KUMPULAINEN<sup>3</sup>, S. RATYNSKAIA<sup>4</sup>, K. PASCHALIDIS<sup>4</sup>, T. RIZZI<sup>4</sup>, P. TOLIAS<sup>4</sup>, L. COLAS<sup>5</sup>, E. LERCHE<sup>5</sup>

<sup>1</sup>ITER Organization, 13067 Saint Paul-lez-Durance, France Email: alberto.loarte@iter.org

### Abstract

This paper describes the evaluations carried out by the ITER Organization and Members' fusion communities to determine the impact of changing first wall (FW) material from beryllium (Be) to tungsten (W) on ITER plasma scenarios and to mitigate such impact, when negative, in the context of the new ITER Research Plan. This includes addition of a boronization system and changes to the heating and current drive (H&CD) systems to increase the coupled power and increasing the proportion of ECH to the mix. In addition, staging of the W FW installation with a temporary inertially cooled FW (TFW) for the first operational campaign to be followed by the final water-cooled FW for DT operation reduces the operational risks while developing scenarios and commissioning control/protection systems.

#### 1. INTRODUCTION

The new ITER baseline includes the change of first wall (FW) material from Be to W [1, 2]. This decision was taken following evaluations of its implications with emphasis on robustness for the implementation of the ITER Research Plan (IRP) and the facilitation of licencing aspects [2, 3, 4]. The main issues identified for the use of Be in ITER concern its toxicity, its limited resiliency to transient loads (chiefly disruptions because of its relatively low melting temperature) and its high erosion rate and subsequent retention of tritium in-vessel. Operation of ITER with a W wall decreases risks associated with these issues but, in turn, introduces additional risks related to the quality of vacuum in ITER (lack of oxygen (O) gettering provided by Be) and plasma contamination by W leading to radiative collapse. The latter is particularly critical since concentrations of W tolerable in ITER plasmas are typically  $\sim$  3 orders of magnitude lower than those for Be and the risk that intolerable W concentrations materialize in ITER needs to be minimized to ensure O > 10 operation.

The new baseline aims at a realistic and robust implementation of the IRP which is divided into three operational phases with increasing plasma performance, fusion power production and neutron fluence targets [3, 4]:

- Start of Research Operation (SRO): well-controlled 15 MA/5.3 T hydrogen L-mode (up to nominal 15 MA/5.3 T plasma current and toroidal field) and deuterium H-mode plasma scenarios (up to 7.5 MA/ 2.65T) with  $P_{ECH} \le 40$  MW,  $P_{ICH} \le 10$  MW and effective disruption mitigation;
- DT-1: DT Q  $\geq$  10,  $P_{fusion}$  = 500 MW,  $t_{burn}$   $\geq$  300s and high-duty operation within a fluence of 3.5  $10^{25}$  neutrons. H&CD:  $P_{ECH} \leq$  60-67 MW,  $P_{ICH} \leq$  10-20 MW and  $P_{NBI} \leq$  33 MW;
- DT-2: to demonstrate the ITER scenario goals, namely advanced inductive operation for pulses longer than 1000s and 3000s at Q  $\geq$  5 in non-inductive steady-state pulses and to assess fusion reactor issues with a neutron fluence of up to 3.0  $10^{27}$  DT neutrons. H&CD:  $P_{ECH} \leq 67$  MW,  $P_{ICH} \leq 20$  MW and  $P_{NBI} \leq 49.5$  MW.

<sup>&</sup>lt;sup>2</sup>Max-Planck-Institut für Plasmaphysik, 85748 Garching bei München, Germany

<sup>&</sup>lt;sup>3</sup>Forschungszentrum Jülich, 52428 Jülich, Germany

<sup>&</sup>lt;sup>4</sup>KTH Royal Institute of Technology, Stockholm, SE-100 44, Sweden

<sup>&</sup>lt;sup>5</sup>CEA, IRFM, 13108 Saint-Paul-lez-Durance, France

<sup>&</sup>lt;sup>6</sup> Laboratory for Plasma Physics, EUROfusion Consortium & TEC Member, 1000 Brussels, Belgium

To strengthen this robustness, in the context of the W wall material change, specific ancillary systems have been introduced (boronization system) [5] or their configuration modified (e.g. increasing coupled power and proportion of ECH vs. ICH in the ITER H&CD radiofrequency mix) [2]. In addition, to minimize the consequences of possible issues in the early development of high current plasmas, a new design of the W FW for SRO operation [2] has been introduced which relies on inertial cooling to minimize the risks of in-vessel water leaks in this phase, during which plasma scenarios will be developed to 15 MA/5.3 T and the associated control and protection systems will be commissioned, including the disruption mitigation system (DMS).

This paper describes the evaluations carried out to substantiate the decision to change the FW material in ITER from Be to W, the new/modified ancillary systems and/or operational strategies adopted in the IRP to mitigate the consequences of this change as well as the key features of the designs for the FW in SRO and in DT-1/DT-2. The evaluations include modelling studies as well as experiments and analysis carried out by ITER Members' fusion institutions including efforts under the International Tokamak Physics Activity (ITPA) for experiments.

### 2. IMPACT OF A W WALL ON VACUUM CONDITIONS AND THE IRP

The use of W as FW material removes the favourable effect of O gettering by Be due to the formation of stable Be oxide. Therefore, a new boronization system (diborane introduction system and additional glow discharge cleaning (GDC) electrodes) has been introduced in the baseline. Modelling studies have been carried out to optimize the distribution of diborane inlet points and GDC electrodes, taking into account installation constraints in ITER [5]. This, together with the phased installation of systems, leads to a very asymmetric distribution of GDC electrodes and thus of boron (B) deposition especially in the SRO campaign (see Fig. 1), with potential risks to the start of operation [1]. Experimental studies have been carried out at WEST [6] and ASDEX-Upgrade [7] to assess the impact of a spatially asymmetric boronization on plasma start-up in all-W devices. These experiments have shown that, while plasma start-up with a W wall without boronization is challenging, the uniformity of boronization plays a lesser role, provided that a sufficient B is deposited to reduce the O levels.

Evaluation of the capacity to trap O in the deposited B layers and their lifetime under erosion has been performed by erosion-deposition modelling [8]. These simulations show that the lifetime of these B layers on the FW is typically  $10^4$  -  $10^5$  s under  $Q \ge 10$  plasma conditions, after which they are either covered by W or deposited at the divertor. Note that up to DT-1 the typical operation pattern for ITER, except for high duty operation [3], considers 13 good pulses per day (2-shift) of typical burn duration 300 s with 12 days of continuous operation (i.e.  $4.7\ 10^4$  seconds of burn), followed by 2 days of short-term maintenance (STM). Thus, application of boronization by GDC in the STM periods allocated every two weeks can be used to refresh the B layers, if needed to maintain good vacuum conditions. It should be noted that coverage of the W wall by B in areas exposed to significant plasma flux is very short lived so that, typically, after few discharges the B layer is completely eroded. This technique is therefore not in any way foreseen to be used as a means for W coverage by B in ITER.

While the boronization system is expected to fulfil its mission, its routine use can lead to significant fuel retention due to co-deposition with eroded B with, typically, 0.1 - 0.3 atoms of hydrogen co-deposited per B atom in metal tokamaks (AUG, C-Mod) [1]. Therefore, specific plasmas (Ion Cyclotron Wall Conditioning (ICWC) and tokamak plasmas) are considered in the IRP to remove this fuel. This includes tokamak plasma operation with the strike point located on B deposits at the divertor (to heat them up and release fuel) followed by ICWC wall conditioning (further details are reported in [1]).

### 3. IMPACT OF A W WALL ON LIMITER AND L-MODE SCENARIOS IN THE IRP

The impact of a W wall on the limiter and low power phases of ITER plasma scenarios has been assessed by experiments and integrated modelling simulations of ITER and present tokamaks in the ITER Members. The main conclusions with regards to the low I<sub>p</sub> phase of ITER scenarios limited on the FW is that W erosion, core W contamination and edge power flow are coupled in a strongly self-regulated system. An increase in W sputtering caused by hydrogen ions or low-medium Z impurities in the plasma, but then typically dominated by self-sputtering, leads to an increased plasma W radiation which, in turn, decreases the plasma edge temperature and power flux on the limiter. This then results in decreased sputtering leading to a stable edge power balance. Extensive SOLPS-ITER simulations of ITER plasmas limited on the FW find radiation fractions in the range of 0.6–0.8 (see Fig. 2) [9]. This is in agreement with initial experimental results in EAST (see Fig. 3) [1, 10] later confirmed by WEST [11] and ASDEX-Upgrade [7] and leads to much lower power fluxes (typically a factor of 2) reaching the ITER FW compared to Be, in which radiation levels of 30% were expected [12]. Contrary to the edge power, full integrated plasma simulations with JINTRAC find that uncontrolled central W accumulation can

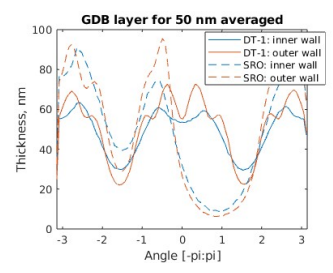


Figure 1. Modelled toroidal variation of the B deposited thickness at the inner and outer midplane showing a factor of 10 variation for SRO and of 3 for DT-1. Diborane reactions in the GDC plasma are modelled and a 20% sticking coefficient is assumed [5].

occur in the absence of central ECH heating due to unfavourable power balance (higher W radiation than local heat transport and source) and neoclassical transport in these ITER plasmas (Fig. 4). This is in agreement with a wider set of modelling studies validated by present experiments [13]. Consistent with this, removing central ECH heating in the limiter phase of EAST experiments led to the radiative collapse of the discharge, as seen in Fig. 3. For L-mode diverted plasmas the use of central ECH heating allows operation with moderate core radiated fractions (<50%) for W wall sources within the typical range in experiments (W gross wall source ~ 10-20 % of the

divertor source [14]), as shown in Fig. 5. We note that for  $I_p \le 15$  MA relatively large W concentrations ( $n_W/n_e > 5 \times 10^{-5}$ ) are compatible with moderate core radiation levels. This is a robust finding [13] and is due to the dominance of electron heating and poor electron-ion coupling in low absolute  $< n_e >$  plasmas (because of low  $I_p$ ) leading to relatively high  $T_e$  ( $\sim 10$  keV) and lower W radiation efficiency.

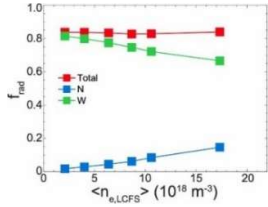


Figure 2. Total fraction of  $P_{heat}$  radiated inside the core (in red) and individual contributions from N (in blue) and W (in green) as functions of electron density at the LCFS obtained in SOLPS-ITER simulations with the 0.5% N concentration and 'prompt redeposition' included [9].

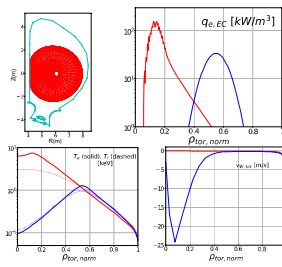


Figure 4. JINTRAC modelling of an ITER plasma in the limiter phase in contact with the WFW at the high field side for two ECH power deposition profiles (on-axis and off-axis). Upper: plasma equilibrium and grid for the plasma modelled and ECH power deposition profiles (red-on axis, blue-off axis). Lower: electron and ion temperature profiles and resulting W pinch velocity (negative values for inwards W fluxes) versus square root normalized toroidal flux for the two ECH power deposition profiles [1].

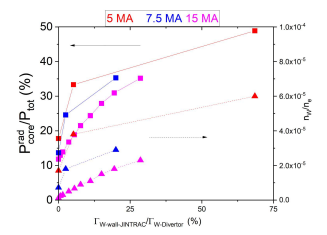


Figure 5. Ratio of core radiated to total heating power and W concentration versus ratio of effective W wall source to divertor source in JINTRAC for L-mode plasmas:  $< n_e > /n_{GW} = 0.3$  for 5 MA,  $P_{ECH} = 5$  MW and 10 MA,  $P_{ECH} = 10$  MW, and  $< n_e > 0.5$   $n_{GW}$  for 15 MA,  $P_{ECH} = 40$  MW.

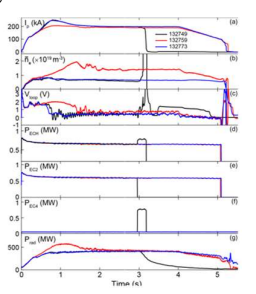


Figure 3. Key time traces for a set of 3 EAST outboard deuterium W limiter plasmas.  $P_{EC2}$  corresponds to central ECH while  $P_{EC4}$  corresponds to peripheral ECH. #132773 and #132749, lowest density with  $n_e/n_{GW} \sim 0.15$  and #132759 at higher density with  $n_e/n_{GW} \sim 0.35$  [1, 10]. Note the radiative collapse of #132749 when central ECH is replaced by peripheral deposition.

## 4. IMPACT OF A W WALL ON H-MODE SCENARIOS IN THE IRP

The impact of a W wall on H-mode scenarios can potentially be more pronounced than on L-mode since a minimum edge power flow must be maintained for the plasma to remain in H-mode. In addition, experiments in tokamaks with W PFCs, especially those with a W wall such as ASDEX Upgrade, show that the edge transport barrier and ELMs play an important role on W production and transport [14]. Although the gross W wall source is much smaller than that from the divertor (typically a factor of 10 less in ASDEX Upgrade) [14,15], it is as effective as the divertor in contaminating the core plasma. Modifying the wall-separatrix gap (thus increasing the W wall source) has a significant impact on the core W concentration and achievable confinement [15]. To confirm whether these findings from ASDEX Upgrade are general or not, a set of experiments were carried out in EAST in which separatrix-W limiter gap scans were carried out in both Type I and II ELMy Hmodes. As discussed in more detail in [3, 10], decreasing the gap has a detrimental effect on plasma confinement and increases radiation in H-modes.

However, these effects are much smaller in Type II than in Type I ELMy H-modes. These experiments highlight that, in addition to wall distance, the outflux by ELMs also plays a key role on the impact of a W wall in H-modes.

Since full integrated modelling of ITER plasmas [16] with the W divertor and FW is not yet possible, two approaches to assess the impact of the W wall on ITER H-modes were followed. For SRO plasmas, in which ELM control in H-modes will be first developed, experimental guidance on the ratio of wall to divertor W source was used, together with results from previous studies on W source modelling by individual ELMs [17], to estimate the magnitude of the W time-averaged ELM-induced influxes. These were compared with full integrated JINTRAC simulations including the divertor W source and an ad hoc W wall source whose magnitude was varied until Hmode confinement was lost by excessive W radiation. The results of these studies are summarized in Figs. 6 and 7 where the time-averaged W influx in the core plasma by ELMs vs. ELM frequency and the resulting core W density and radiation in 5 MA/2.65 T SRO H-mode plasmas is evaluated. These simulations show that if the ELM frequency is maintained sufficiently high (typically above 30 Hz), the time-averaged W wall influxes caused by ELMs in ITER should be compatible with H-mode operation in SRO. ELM resolved integrated simulations [3, 16] indicate that the instantaneous core radiation peak caused by W influxes from ELMs can lead to a transient loss of H-mode, thus the requirements for ELM control derived from these time-averaged W influxes may not be sufficient to avoid transient H-L transitions. For this reason, the ITER configuration for SRO includes the full set of ELM control coils as well as four pellet injectors providing the potential for ELM triggering with a frequency up to 60 Hz. We note that the experimental plan in SRO considers scans of the separatrix-W wall gap (within TFW power flux/energy design limits) to assess the W contamination issue as well as to demonstrate that the requirements for ELM control in DT-1 (small/no ELM H-modes) can be achieved [3, 4].

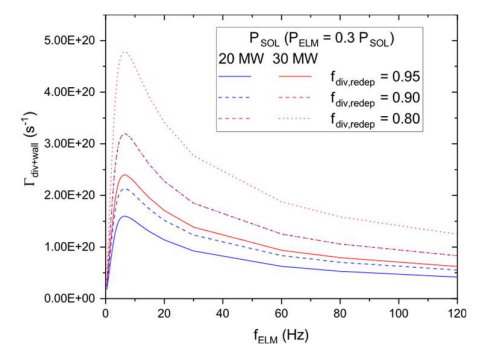


Figure 6. Modelled time-averaged W influx by ELMs into the plasma from the divertor and the main wall versus ELM frequency for typical edge power levels of SRO H-mode operation in ITER and a range of assumptions regarding prompt divertor re-deposition [3]. The W influx is calculated on the basis of the modelling results for the gross W source in [17].

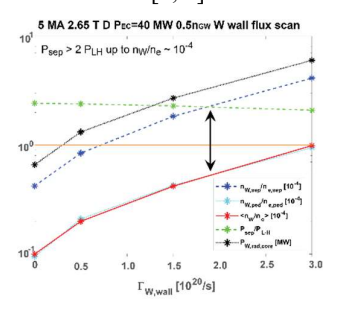


Figure 7. Modelled W concentrations at the separatrix, pedestal top, core plasma, core W radiation and margin of the edge power flow to the L-H transition versus time-averaged W wall source by ELMs for 5 MA/2.65  $T < n_e > = 0.5 \ n_{GW} \ D$  H-mode plasmas with  $P_{ECH} = 40 \ MW$ . The double-headed arrow shows the difference between separatrix W concentration (in blue) and core/pedestal W concentration (in cyan/red) due to W screening in the pedestal [3].

For DT-1 plasmas, the impact of the W FW on high Q operation has been evaluated under the assumption that an H-mode plasma scenario without ELMs has been developed in advance (e.g. by application of 3-D fields or alternatives such as QCE, X-point radiator, QH-mode, etc.). In terms of modelling assumptions, the so-called continuous ELM model is applied, which describes pedestal transport by adjusting anomalous diffusion to provide stationary pedestal parameters without ELMs. For W, neoclassical transport (diffusive + convective) in the pedestal is considered in addition to anomalous diffusion. This, together with the requirement of a sufficiently high separatrix density for divertor power exhaust in high Q scenarios, results in W being screened by the high temperature gradients/low density gradients in the pedestal and results in a W core density significantly lower than at the separatrix, as shown in Fig. 8 for typical  $Q \ge 10$  plasmas. Such conditions with edge W screening are infrequent in present experiments because of the high edge ion temperature gradients required. When these conditions are met, experimental results from JET have shown that W screening can be observed [18].

While screening is favourable to reduce the impact of W influxes into the ITER core plasma and to maintain the required performance for  $Q \ge 10$ , this does not imply that such performance can be sustained under an arbitrary increase of W influxes into the plasma driven by a W wall source. To quantify the impact of W wall influxes on high Q plasmas, a series of studies has been carried out to determine the W wall influxes from erosion/deposition models on the basis of modelled ITER SOL plasmas. These results have been used as input to an ad-hoc model for a W wall-source in the integrated-model JINTRAC to evaluate the consequences of the W wall fluxes for core plasma performance. The first attempts at this approach were based on existing SOLPS+OEDGE solutions and

WallDYN2D modelling [8]. Recently a more self-consistent approach has been followed by the use of the widegrid SOLPS-ITER code with ERO2.0 modelling and JINTRAC with the same assumptions regarding SOL transport. Although details vary with the approach followed, the key results are similar: a) the main mechanism for W production from the FW is sputtering by Ne (required for divertor power exhaust), with charge-exchange sputtering by D/T neutrals playing a secondary role, and b) for the highest W wall influxes core radiation increases to values  $\sim 80$  MW. To sustain H-mode performance and  $P_{\text{fusion}} = 500$  MW under these conditions, an increase of the additional heating power up to 70 - 90 MW (compared to 50 MW for  $Q \ge 10$  operation) is required with the corresponding impact on the resulting Q, as shown in Fig. 9. While the IRP foresees that, with progress of R&D, the control of W influxes and resulting impact on performance will be demonstrated to achieve  $Q \ge 10$ , it can be expected that in the transient H-mode phases and in the first attempts at high Q operation, core radiation fractions of ~ 50% maybe reached with a W wall, as it was the case in initial JET operation with a W divertor and in ASDEX Upgrade unboronized plasmas [15, 19]. As a consequence, and to provide flexibility to the IRP, an additional 20 MW of ECH is installed in the post-SRO shutdown to provide increased central heating. We note that in these ITER plasma conditions, uncontrolled peaking of the core W profile by neoclassical transport effects, frequently seen in many of today's experiments [13], is not found when increasing W influxes. The limiting process driven by excessive W influxes is the loss of the H-mode regime [3, 13]. This different behaviour is caused by the dominance of anomalous W transport over neoclassical transport in the core of ITER H-mode plasmas. Specific studies that validate this prediction on the basis of present experiments are reported in [13].

In addition to these studies including the application of NBI and ECH for high Q operation, specific assessments have also been carried out for ICH. This concerns the potentially increased W source due to the edge electric fields paralel to the magnetic field  $(E_{\parallel})$  created by RF heating. This is seen in some experiments with non-optimized antennae because of large  $E_{\parallel}$  at surrounding or nearby W PFCs [20]. This can be avoided by the choice of phasings and current levels in the antenna straps to minimize these fields (3-strap antenna in ASDEX Upgrade) and, thus, reduce W sputtering. Studies in [20, 21] have shown that the ITER ICH antenna has sufficient flexibility to reduce the electric field to ASDEX Upgrade-like values resulting in an ICH-driven W wall source of, at most, a few  $10^{19}$  s<sup>-1</sup>, as shown in Fig. 10. This is typically one order of magnitude lower than the W wall source due to plasma-wall interactions for  $Q \ge 10$  plasmas [8] and is thus not expected to impact core W concentration. Following confirmation of these findings in SRO, the ICH system will be upgraded to provide 20 MW of power in DT-1 [2].

### 5. BASIS FOR THE DESIGN OF THE TUNGSTEN FIRST WALL FOR SRO AND DT OPERATION

The new baseline includes two FW's: a temporary inertially-cooled wall (TFW) for SRO [22] and the final watercooled wall for DT-1. Both include W as plasma-facing material, but, because they are associated with the specific objectives of these phases in the IRP, their design bases are very different. The SRO TFW is designed to accommodate loads from plasmas up to 15 MA/5.3 T with high power heating (~40 MW) for flat-top durations of few tens of seconds while providing resiliency to transient loads that may occur due to insufficient control/mitigation in this first campaign (e.g. disruptions, VDEs, runaway electron (RE) impact) [1, 3]. The TFW has a geometry as close as possible to the final water-cooled DT-1 FW and is inertially cooled, so that uncontrolled loads leading to TFW melting will not cause in-vessel water leaks (note that the full set of blanket shield blocks will be installed already for SRO, but will not be water-cooled in this first phase). To optimize the cost of the TFW, while maintaining its objectives, a choice of W coatings, W-alloys and bulk W (as shown in Fig. 11) is being considered for various regions of the wall depending on the expected loads, while the design allows for any choice at all locations. To define these loads, a range of ITER scenarios have been modelled with free-boundary codes, as shown in in Fig. 12, and with integrated models covering a range of assumptions regarding the W concentration in the core plasma, etc., to determine the power fluxes to the TFW panels [22]. The results of these simulations indicate that stationary plasma conditions can be reached within  $\sim 10$  - 20 s of the start of the flat-top main heating phase. Thus, a heating phase duration of ~ 30 - 50s, depending on heating power level, is taken as a guideline for the TFW design. These considerations, together with those of cost optimization, lead to a choice of TFW materials with W coatings for the areas subject to low or short-lived plasma flux and bulk W for the rest. Regarding bulk W, the choice of pure W versus W-alloys panels, which are easier to manufacture and of lower cost, depends on the likelihood that a specific TFW panel will receive loads during disruptions. The medium Z components in W alloys (e.g. W (wt.%) 97, Ni (wt.%) 2, Fe (wt.%) 1) melt at much lower temperature (1500°C) than bulk W (3420 °C) and, thus, these alloys are less resilient to disruptions. In this respect, for SRO, the invessel vertical stability control coils will be used to minimize the risk of downwards going plasmas during disruptions. This avoids heavy transient heat fluxes and RE deposition on the final actively cooled divertor. This leads to the choice of bulk W with higher disruption resilience for the rows of TFW panels 6 to 11. The TFW panels in row 18 are also made of bulk W to account for the sporadic cases in which the displacement of the plasma during disruptions is downwards. The rest of the TFW panels are W coated except those in rows 3 to 5, which are directly exposed to plasma contact in the limiter start-up phase; these are made of W alloys since they

are not expected to be subject to large transient loads. Initial estimates with 2-D modelling indicated that melting of the bulk TFW panels (except leading edges) during the current quench (CQ) of disruptions in SRO would be avoided up to, at least, 10 MA/5.3 T, providing a wide a wide operational space to characterize disruption loads and to develop their mitigation [1, 3]. New non-linear resistive MHD simulations including 3-D effects, and validated against JET experimental data, indicate that the operational space without large scale W melting during the CQ of disruptions could be wider, reaching up to 15 MA [23]. As shown in Fig. 13, under such conditions, there is some localized melting in TFW rows 7-11 with most of the energy being deposited on panels 7-9. The high power fluxes on TFW rows 10 and 11 are associated with panel design issues being presently examined to minimize melting there. If these modelling results are confirmed in SRO, they will open the way to a less demanding optimization for the DMS as well as for the characterization of unmitigated disruption loads up to 15 MA, if electromagnetic forces on vacuum vessel and in-vessel components allow.

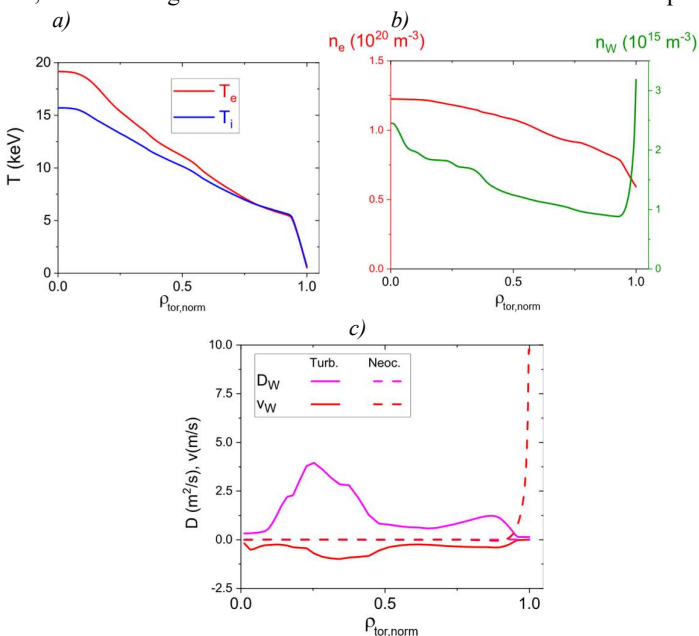


Figure 8. JINTRAC modelled core and pedestal plasma parameters and W transport coefficients versus square root normalized toroidal flux for  $Q \geq 10$  plasmas modelled with the core transport model TGLF-SAT2 and the continuous ELM model for pedestal transport : a) electron and ion temperatures, b) electron and W densities and, c) W transport coefficients (diffusion and pinch velocity) showing the reduction of anomalous transport in the pedestal and dominance of the outwards neoclassical W pinch and the absence of significant core peaking for the W density due to the dominance of turbulent diffusion.

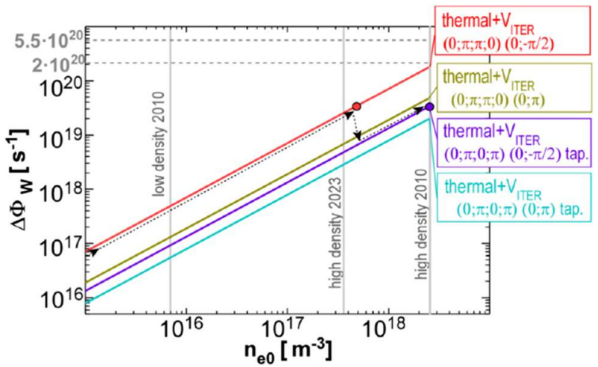


Figure 10. ICH-specific W sputtering rate for  $P_{ICRF} = 10$  MW as a function of the density at the PFCs surrounding the antenna  $(n_{e0})$  for  $Q \ge 10$  plasmas. Due to uncertainties in far-SOL particle transport in ITER,  $n_{e0}$  spans a large range of values [20].

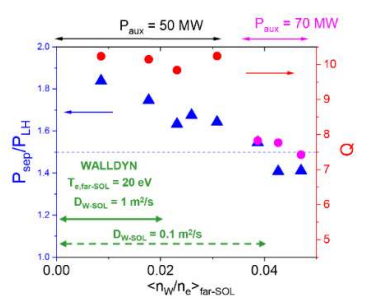


Figure 9. JINTRAC modelled Q and margin of edge power flow above the L-H transition versus average W density in the far-scrape-off layer (SOL) compared to predictions from WallDYN2D for 15 MA/5.3 T DT plasmas with additional power heating levels of 50 MW ( $Q \ge 10$ ) and 70 MW for the highest W edge density/wall influx range.

In addition to resilience to thermal loads (thermal quench, CQ) during disruptions, W also has a much higher stopping power for REs. This helps to minimize the risks that formation of multi-MA RE beams during disruptions pose to ITER's availability for scientific exploitation in DT-1. This risk concerns water leaks that can be triggered by a too high temperature

at the FW panel cooling interface and, thus, is not relevant for SRO.

To evaluate the implications of RE impact on a water-cooled FW panel in DT-1 a series of studies [24] have been carried out with the Geant4 Monte Carlo (MC) code simulating the volumetric energy deposition MEMENTO heat transfer simulations of the PFC thermal response taking the input RE parameters from DINA and JOREK simulations. These include short (~ 1 ms) and long terminations (~ 100 ms) with significant conversion of magnetic to kinetic RE energy. The results show that, in terms of surface damage, the FW panel W armour thickness (typically  $\geq 8$  mm) does not have much impact. For long terminations with large magnetic energy conversion increasing the thickness reduces the risk of a leak developing.

This risk is quantified by the temperature of the W-CuCrZr interface of the FW panel with the cooling channel reaching 1000-1200 K (CuCrZr melts at 1350°C), as shown in Fig. 14. It is important to note that for very large RE deposited energies the amount of melted and vaporized material reaches several mm so that the resilience of

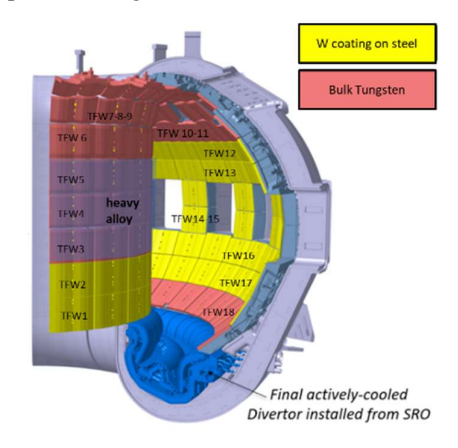


Figure 11. TFW for SRO showing the specific choice of plasma-facing material (W coating, bulk W or W alloy) depending on the expected loads during SRO scenarios.

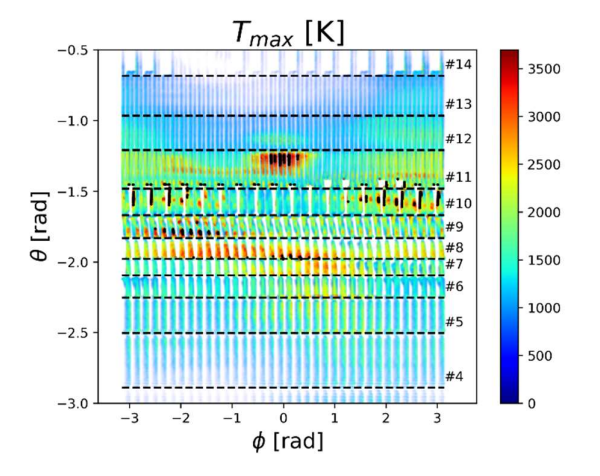


Figure 13. Maximum surface temperature on the ITER TFW panels during a 15 MA unmitigated upwards VDE. The FW surface is represented in toroidal  $(\phi)$  and poloidal  $(\theta)$  coordinates, with the poloidal index of the FW panels (#). Black dots mark elements where the surface temperature exceeds the W melting point [23].

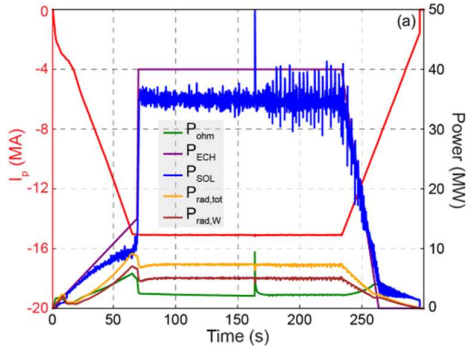


Figure 12. End-to-end DINA scenario for a hydrogen L-mode to 15 MA at 5.3 T: main components of the power balance with the  $I_P$  waveform – the oscillations on  $P_{SOL}$  from t ~164 s are due to sawteeth. Note that this scenario takes no consideration of energy limits on the FW and that a range of radiation powers from 20-50 % is considered for the design [1].

the FW panels to multiple events of this large magnitude is low. On the basis of these results and additional engineering considerations, the thickness for the areas of the W water-cooled DT FW most likely to be subject to RE impact has been increased to 12 mm compared to 6 mm elsewhere.

The results of the studies in [24] are summarized in Fig. 15 by identifying the maximum RE current leading to a leak in a single event as a function of the energy deposited on a FW panel with 12 mm thick W armour and of the sharing among FW panels in a row, for both short and longer RE deposition. For fast events, if the RE load is shared among many FW panels, up to 9 MA of RE current could be acceptable without (marginally) causing a potential water leak. For slower events this is in the range of 2 - 4 MA if RE deposition is toroidally uniform. Therefore, although the use of W provides some increased resilience of the FW to single RE events compared to Be, effective RE avoidance/mitigation remains mandatory in DT-1 and its development is one of the main objectives

of SRO together with the inertially cooled TFW, which avoids this risk by design (no water cooling).

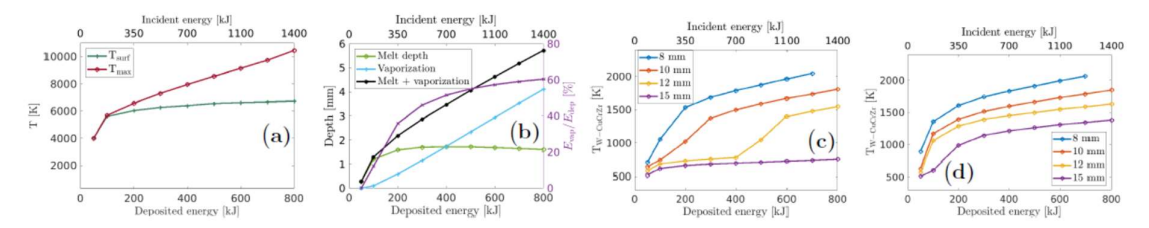


Figure 14. Surface damage (a-b) and cooling system response (c-d) per apex of FW panel in the upper main chamber (2 apexes per panel and 18 panels per toroidal row) for a DINA scenario with 100 ms RE loading. The temperature at the W-CuCrZr interface is shown for the Critical Heat Flux (CHF) at 30MW/m² in (c) and 10MW/m² in (d) [24].

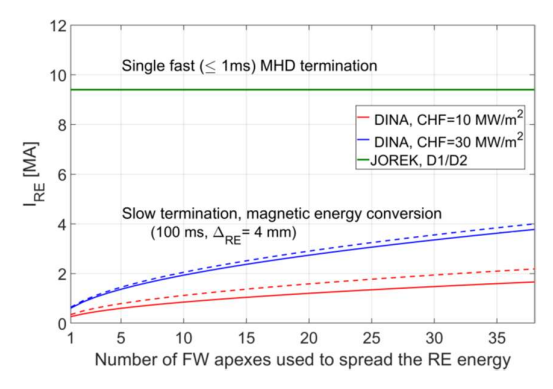


Figure 15. Damage thresholds, expressed as RE current values at which  $T_{W-CuCrZr}=1000~K$  (full lines) or  $T_{W-CuCrZr}=1200~K$  (dashed lines) is reached for a 12 mm W thickness. The calculations of curves corresponding to DINA scenarios are based on: (i) total incident energy scales as  $E_{inc}\sim I_{RE}^2$  as per magnetic energy conversion, (ii) for  $I_{RE}=9.4~MA$ ,  $E_{inc}=200~MJ$ , as obtained from JOREK simulations and (iii) the total RE energy is evenly spread among the FW apexes. The green curve corresponds to the RE current that would produce  $T_{W-CuCrZr}=1000~K$  in the case of the single fast MHD termination simulated by JOREK [24].

### 6. SUMMARY

This paper summarizes the evaluations carried out by the ITER Organization and ITER Members' experts, working under the ITPA framework for coordinated experiments, in support of the decision to change the first wall material from Be to W in the new baseline, as well as to stage the installation of the W wall with an inertially cooled wall in SRO and the final water-cooled wall in DT-1.

The risks associated with this change have been quantified and mitigated by the installation/modification of new/existing systems. These include: a new boronization system to obtain good vacuum conditions for plasma start-up and an increase of the overall heating power for DT operation (from 73 MW to 103/120 MW) with increased sharing of ECH (40/47 MW increase) compared to the previous baseline. This provides operational flexibility for the initial development of scenarios in which high W core radiation levels are expected and also supports the achievement of the  $Q \ge 10$  goal with low neutron fluence by interleaving D and DT operation [3,4]. In addition, the suitability of ICH heating with a W wall has been analyzed and found to be compatible with acceptable W influxes.

Following confirmation in SRO, the ICH system will be upgraded to 20 MW for operation in DT-1. Finally, the choice of W for the FW increases its resilience to disruption loads. This, together with inertial cooling in SRO, facilitates the commissioning with plasma of the DMS to demonstrate efficient disruption mitigation up to 15 MA and will enable the characterization of unmitigated disruption loads up to 10 - 15 MA, if electromagnetic loads on the vacuum vessel and in-vessel components allow. With regards to DT-1, the use of W with a thickness of 12 mm in the disruption loaded areas increases the resilience of the FW to RE loads compared to Be by decreasing the likelihood of single-event failure (water leaks). However, as it was the case for a Be FW, routine RE mitigation/avoidance remains mandatory for ITER DT operation with a W FW.

### **ACKNOWLEDGEMENTS**

The fusion communities in the ITER Members and the scientists involved in ITPA activities are gratefully acknowledged for the strong support provided to the ITER Organization. Thanks to this support it has been possible to conduct the assessments described in this paper in a timely manner to support the ITER FW strategy and the associated changes in ITER systems/components adopted for the new baseline. The views and opinions expressed herein do not necessarily reflect those of the ITER Organization.

### REFERENCES

- [1] R.A. Pitts, et al., Nuclear Materials & Energy 42 (2025) 101854.
- [2] P. Barabaschi, et al., this conference.
- [3] A. Loarte, et al., 2025 Plasma Phys. Control. Fusion 67 065023.
- [4] S. W. Yoon et al., this conference.
- [5] T. Wauters, et al., Nuclear Materials and Energy 42 (2025) 101891.
- [6] E. Geulin, et al., this conference.
- [7] J. Hobirk, et al., this conference.
- [8] K. Schmid, et al., Nuclear Materials and Energy 41 (2024) 101789.
- [9] Y. Zhang, et al., 2025 Nucl. Fusion 65 056035.
- [10] X. Gong et al., this conference
- [11] P. Manas, et al, Proc. 51st EPS DPP Conference, Lithuania
- [12] R.A. Pitts, et al., 2022 Nucl. Fusion 62 096022
- [13] D. Fajardo, et al., this conference.

- [14] R. Dux, et al., 2011 Nucl. Fusion 51 053002.
- [15] R. Dux, et al., Journal of Nuclear Materials 390-391 (2009) 858.
- [16] M. Schneider, et al., this conference
- [17] R. Dux et al., Nuclear Materials and Energy 12 (2017) 28.
- [18] A.R. Field et al., 2023 Nucl. Fusion 63 016028.
- [19] E. Joffrin, et al., 2014 Nucl. Fusion 54 013011.
- $[20]\ V.$  Bobkov, et al., Nuclear Materials & Energy 41 (2024) 101742.
- [21] L. Colas, et al., Nuclear Materials & Energy 42 (2025) 101831.
- [22] L. Chen, et al. Proc. 20th PFCM Conference, 2025, Slovenia.
- [23] S. Carpentier, et al., 33rd SOFT conference, 2024.
- [23] F.J. Artola, et al., this conference.
- [24] S. Ratynskaia, et al., sub. PPFC, https://arxiv.org/abs/2509.20261.